



# Evaluation of the use of magnetic sector secondary ion mass spectrometry to investigate $^{14}\text{C}$ distribution in Magnox reactor core graphite

LIAM PAYNE\*, PETER J. HEARD AND THOMAS B. SCOTT

Interface Analysis Centre, University of Bristol, Bristol, BS8 1TL, United Kingdom

[Received 18 August 2014; Accepted 14 February 2015; Associate Editor: Katherine Morris]

## ABSTRACT

Large quantities of irradiated graphite will arise from the decommissioning of the UK's Magnox power stations. Irradiated graphite contains  $^{14}\text{C}$  as well as other longer lived radionuclides (e.g.  $^{36}\text{Cl}$ ). The potential use of magnetic sector secondary ion mass spectrometry (MS-SIMS) to examine the distribution of the  $^{14}\text{C}$  within trepanned graphite samples from a Magnox nuclear power station has been investigated. This work indicates that the methodology proposed has the potential to be used to analyse irradiated graphite samples with preliminary results highlighting a possible  $^{14}\text{C}$  enrichment in the carbonaceous deposit found on a channel wall sample.  $^{14}\text{C}$  concentrations in samples without this deposit were below the limits of detection of the instrument. The methodology used for these determinations ensured that possible mass interferences between  $^{14}\text{C}$  species and oxygen-bearing or nitrogen-bearing species were eliminated from the analysis. Future work will utilize the methodology proposed in this work on a larger number of samples.

**KEYWORDS:** graphite, Magnox reactor,  $^{14}\text{C}$  distribution, magnetic sector secondary ion mass spectrometry, MS-SIMS.

## Introduction

THE decommissioning of the first generation of gas-cooled, graphite-moderated reactors in the United Kingdom will lead to approximately 45,000 m<sup>3</sup> of irradiated graphite waste requiring disposal (NDA, 2013). The majority of this will be classified as intermediate level waste (ILW) (NDA, 2014) due to its content of the long-lived radionuclide  $^{14}\text{C}$ , which is a significant radionuclide for consideration in the safety case for a geological disposal facility (GDF) in the UK (NDA, 2012). Carbon-14 has a sufficiently long half-life (5730 years), allied

with the potential for formation of gaseous species, for its release to be of relevance after closure of a GDF (Baston *et al.*, 2012). An improved understanding of the distribution of this radioisotope in irradiated graphite, its chemical form and possible rates of release are therefore of importance (Baston *et al.*, 2014).

This work investigates whether the use of magnetic sector secondary ion mass spectrometry (MS-SIMS) is suitable to determine the distribution of  $^{14}\text{C}$  in irradiated graphite samples trepanned from one of the reactor cores at Oldbury Magnox power station (Gloucestershire, UK) in 2004, after 37 years of operation. The typical method for determining  $^{14}\text{C}$  in irradiated graphite is destructive, whereby samples are degraded (Takahashi *et al.*, 1999), either thermally or with solvents, and

\* E-mail: liam.payne@bristol.ac.uk  
DOI: 10.1180/minmag.2015.079.6.08



The publication of this research has been funded by the European Union's European Atomic Energy Community's (Euratom) Seventh Framework programme FP7 (2007–2013) under grant agreements n°249396, SeclGD, and n°323260, SeclGD2.

the  $^{14}\text{C}$  released is measured. MS-SIMS inflicts minimal damage on the specimen in very small regions, and therefore, if this technique could be validated, it could be used to examine the distribution of  $^{14}\text{C}$  in irradiated graphite and aid the understanding of results achieved from future microbial leaching experiments.

## Experimental

### *Instrumental approach to analysis*

An in-house-built MS-SIMS, Fig. 1, was used throughout this work. Full details of the system are described elsewhere (Heard *et al.*, 2002). The system comprised a focused gallium ion gun (FEI electronically variable aperture type) fitted to a Vacuum Generators model 7035 double-focusing magnetic sector mass analyser with a channeltron ion detector. The equipment was controlled using software that was written in-house (*PISCES*, Dayta Systems Ltd., Thornbury, UK). The bombardment of samples by the primary gallium ion beam leads to the release of a range of secondary particles including positive ions, negative ions, neutral particles, multiple particles and electrons (Magee and Honig, 1982).

The system has the capability of being used in four main operational analysis modes: secondary electron imaging; survey spectrum acquisition;

depth profiling; and secondary ion mapping. For the three mass spectrometry modes, the system can work in either positive or negative ion counting modes. The system is equipped with an Everhart-Thornley electron detector ensuring that secondary electron images of a sample can be obtained at spatial resolutions determined by the diameter of the ion beam (Heard *et al.*, 2002). This allows visualization of the surface of the sample and identification of possible surface features.

Survey spectra were obtained by raster scanning the ion beam over an area of interest, usually at low magnification to limit the damage caused to the specimen by the ion beam, and scanning through the mass range of interest. In the present work, the scanned range was from 0–100 Daltons (Da) at 0.05 Da steps with a duration of 100 ms per step. This allowed the precise mass-to-charge ratio ( $m/z$ ) of the species of interest to be identified, ensuring the maximum possible signal was achieved.

For the majority of the present work, the depth profiling capability of the MS-SIMS system was employed in negative ion mode. In this mode of operation the ion beam was repeatedly raster scanned over a small region of the sample. This slowly ablated the sample surface, creating a box-shaped crater whilst simultaneously recording the signal intensity from one or more selected ion species. Depth profiling is used routinely to detect variations in composition with depth below the surface of

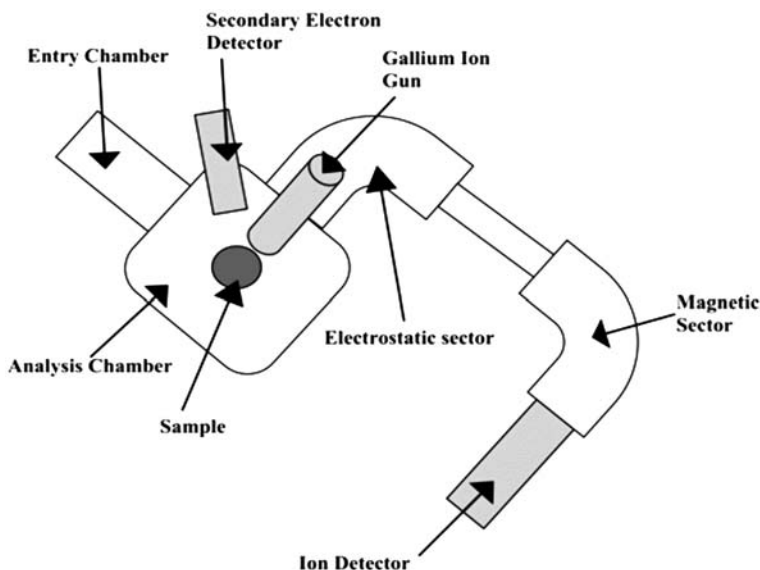


FIG. 1. Schematic diagram of MS-SIMS instrument.

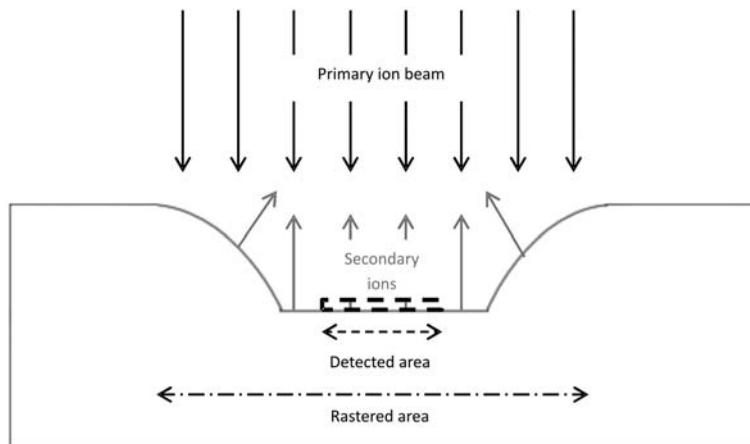


FIG. 2. Schematic diagram showing the principle of electronic gating used during depth profiling.

specimens and is ideal for the studies of coatings and their buried interfaces. Here the facility was used to initially remove surface contamination and then to continue monitoring species of interest with increasing penetration depth into the sample, integrating the signal over time in order to improve ion counting statistics.

Although SIMS has several benefits over other surface analytical techniques, notably the ability to separate elemental isotopes, it does have some operational limitations that need consideration.

Firstly, during depth profiling there is the possibility that the crater edges will cause sidewall contributions that have the potential to affect results. To minimize this, electronic gating was utilized throughout this work, in which the beam was raster scanned over an area but secondary ions were only collected from a reduced area within the crater (Fig. 2); this minimized crater edge effects.

Secondly, SIMS analysis is routinely performed on flat samples as it can be affected by topographical variations as well as by sample geometry (Lee *et al.*, 2011). This is primarily due to the non-uniform sputtering behaviour of non-flat samples that can lead to variations in the energy and emission angle of emitted secondary ions (Lee *et al.*, 2011). The graphite samples studied in this work had non-uniform, irregular surfaces and therefore they were likely to exhibit effects that hinder data interpretation and quantification. The ion signals were therefore normalized to the  $^{12}\text{C}$  signal in the sample, as in equation 1,

$$r = \frac{S_1 - B}{S_2 - B} \quad (1)$$

where:  $r$  is the normalized signal,  $S_1$  is the signal of the secondary ion species of interest,  $S_2$  is the signal arising from  $^{12}\text{C}$  and  $B$  is the background signal.

Finally, there is the possibility that two (or more) secondary ion species have mass to charge ratios that are too close together for the instrument to resolve between them. For the current work there is an isobaric interference between  $^{14}\text{C}^-$  ( $m/z = 14.003$ ) and  $^{12}\text{CH}_2^-$  ( $m/z = 14.016$ ), this would require a mass resolving power (MRP) of 1077 to separate the peaks. It was not possible to use the  $^{14}\text{C}^-$  signal directly to measure the  $^{14}\text{C}$  content as the instrument used has a low MRP compared to commercial instruments. However, the instrument is able to handle radioactive samples unlike most commercial SIMS instruments in the UK. In light of this the  $^{12}\text{C}_2^-$  species at  $m/z = 24$  and  $^{14}\text{C}_2^-$  species at  $m/z = 28$  were used for the  $^{12}\text{C}$  and  $^{14}\text{C}$  assessment, respectively. There is, however, a further possibility of isobaric interferences at  $m/z = 28$  from  $^{14}\text{C}^{14}\text{N}$ ,  $^{14}\text{C}^{12}\text{CH}_2$ ,  $^{28}\text{Si}$ ,  $^{13}\text{C}^{15}\text{N}$ ,  $^{13}\text{C}^{14}\text{N}^+\text{H}$  and  $^{12}\text{C}^{16}\text{O}$  that would require an even greater MRP to separate, however this work does not aim to resolve the peaks but rather correct for possible contributions to the signal at 28 Da. Such a correction would be difficult to perform at 14 Da as the signal arising due to  $\text{CH}_2$  would be very dominant. Experiments were performed in order to assess the magnitude of the signal from  $^{12}\text{C}^{16}\text{O}$  by deliberately introducing oxygen into the system to generate such species, and monitoring the  $m/z = 28$  signal as a function of the oxygen signal at  $m/z = 16$ . The contribution due to  $^{14}\text{C}^{14}\text{N}$  was subtracted by measuring the signal at  $m/z = 26$  ( $^{12}\text{C}^{14}\text{N}$ ) and

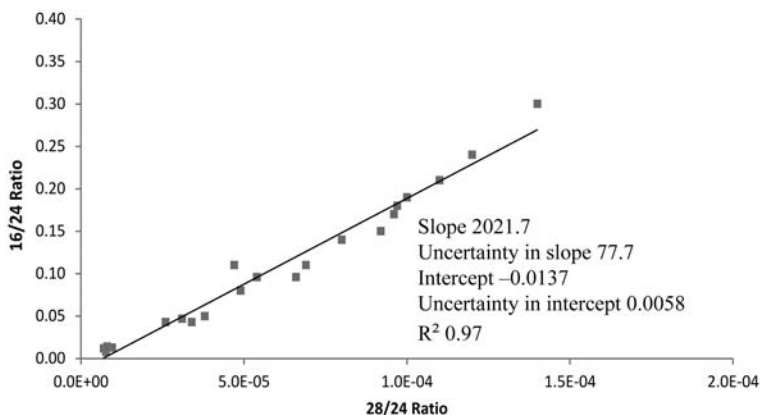


FIG. 3. The relationship between the 28/24 and 16/24 normalized signal ratios for virgin PGA exposed incrementally to oxygen during analysis. The  $m/z = 28$  signal is assumed to be from  $\text{CO}^-$  species generated on the surface. Inset shows values from regression analysis performed by Origin.

calculating the relative contribution to the signal at 24 and then applying this factor,  $k$ , to results obtained, equation 2,

$$k = \frac{(C - B)}{(C - B) + (N - B)} \quad (2)$$

where:  $k$  is the correction factor applied to the results,  $C$  is the signal arising at  $m/z$  24,  $N$  is the signal arising at  $m/z$  26 and  $B$  is the background signal at  $m/z$  27.6

### Sample provenance and preparation

Irradiated pile grade A (PGA) graphite samples trepanned from the core of Reactor One of Oldbury

power station were examined. A cylindrical trepan of approximately 20 mm long was cut into three slices by the National Nuclear Laboratory (NNL), giving a total of six sample surfaces to be analysed, front and reverse of each slice. No further preparation was performed before analysis. These samples consisted of one face that was exposed to the fuel/interstitial channel of the reactor, channel wall face, and five that originated from within the bulk of the graphite, inner brick. Virgin (PGA) graphite material, which was surplus from the commissioning of Wylfa power station (Anglesey, Wales), was provided by Magnox Ltd. to act as a comparator. This material was machined using a diamond cutting wheel, South Bay Technology Inc.

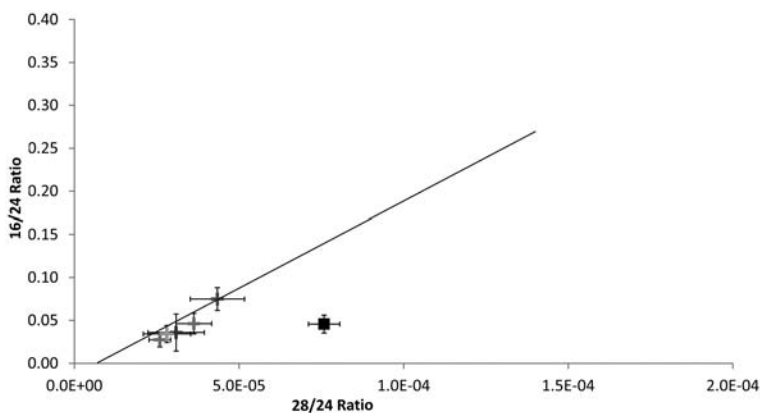


FIG. 4. Comparison of 28/24 to 16/24 ratios for a set of trepanned graphite samples (square shows channel wall face and crosses show inner brick samples). Solid line is from Fig. 3.

TABLE 1 Mean signal counts and standard error of the mean for six areas of the channel wall face deposit on an irradiated sample.

|        | m/z 24        | m/z 28    | m/z 16      | m/z 26        | m/z 27.6 |
|--------|---------------|-----------|-------------|---------------|----------|
| Area 1 | 934931 ± 474  | 94 ± 0.7  | 66547 ± 356 | 573038 ± 1546 | 15 ± 0.2 |
| Area 2 | 825355 ± 809  | 68 ± 0.6  | 65655 ± 223 | 417807 ± 456  | 7 ± 0.2  |
| Area 3 | 788476 ± 979  | 56 ± 0.4  | 27717 ± 94  | 418850 ± 506  | 10 ± 0.2 |
| Area 4 | 842093 ± 1521 | 68 ± 0.6  | 36110 ± 110 | 469987 ± 639  | 9 ± 0.2  |
| Area 5 | 703924 ± 1695 | 67 ± 0.6  | 24919 ± 34  | 511861 ± 474  | 14 ± 0.2 |
| Area 6 | 925867 ± 3422 | 117 ± 1.4 | 9718 ± 67   | 609577 ± 1559 | 31 ± 0.5 |

Model 650, with deionized water as coolant to give specimens of matching dimensions to the trepanned irradiated samples. Due to the nature of the irradiated graphite samples exact replica sample preparation was not possible as irradiated samples were prepared by NNL before receipt; however it is not believed this will affect the results. All samples were analysed in custom-made leaded-brass analysis stubs, which supported the samples without the use of adhesives while offering some radiation shielding. Additionally, survey spectra from a 60  $\mu\text{Ci}$   $^{14}\text{C}$  check source were acquired to verify the presence of a signal at m/z 28 due to  $^{14}\text{C}_2^-$ .

### Analytical methods

All analyses were performed in negative ion mode with a gallium ion beam current of 3 nA and an ion energy of 25 keV. The sample potential was held at approximately -4 kV.

### Survey spectra

Survey spectra from each sample face were acquired by scanning the ion beam over an area of  $400 \times 300 \mu\text{m}$  and scanning a mass range of 0–100 Da with 0.05 Da steps and a dwell time of 100 ms per step. The data were used for initial peak identification and instrument calibration.

### Depth profiles

Depth profiles were acquired from six equal sized areas of each sample face, choosing sites that generated sufficient secondary ion emission for analysis. A lack of secondary ion signal is due to limited manipulation of the sample analysis stage of the instrument. These were acquired by scanning the ion beam over an area of  $65 \mu\text{m} \times 55 \mu\text{m}$  and

detecting secondary ions over a gated area of approximately  $20 \mu\text{m} \times 15 \mu\text{m}$ . Profiles were collected for 1800 seconds, with the average signal intensity calculated between 200–1800 s and subsequently used in the calculation of normalized signal ratios. Data from the first 200 s were discarded. This was in recognition of surface contamination layers, which it was assumed would be removed at the end of such a timescale. Signals from five mass peaks were recorded during analysis, at m/z values of 16, 24, 26 27.6 and 28. These correspond to atomic oxygen, carbon-12, carbon-nitrogen, background and carbon-14 respectively. The background signal was recorded in an area where no mass peaks are anticipated to occur, 27.6. This allows a baseline subtraction of extraneous signals arising from the instrument. Two normalized signal ratios were calculated; 28/24 for comparison of  $^{14}\text{C}$  to  $^{12}\text{C}$ , and 16/24 to investigate the presence of oxygen so that any  $\text{CO}^-$  interference could be subsequently corrected for.

### Oxygen investigation

Investigation into possible  $\text{CO}^-$  interference at m/z = 28 was performed by collecting similar depth profiles from virgin PGA graphite. The graphite was incrementally exposed to research grade oxygen during analysis from a total chamber pressure of  $2 \times 10^{-8}$  mbar up to a maximum chamber pressure of  $1 \times 10^{-6}$  mbar (and then returned to base pressure) in order to deliberately generate  $\text{CO}^-$  species on the sample surface. From base pressure, the first increase in pressure occurred at 500 s, and each subsequent pressure change was at approximately 300 s intervals over a total acquisition time of 3600 s. A steady 200 s period of stable pressure where reliable data could be acquired was therefore provided. The results allowed a measurement of the normalized 28/24

ratio that would arise from  $\text{CO}^-$  species alone, enabling  $\text{CO}^-$  contributions to the  $m/z = 28$  peak to be corrected for in subsequent experiments on the irradiated samples.

## Results

### Oxygen investigation

The calculated 28/24 and 16/24 normalized signal ratios at different oxygen pressures are shown in Fig. 3 with values and uncertainties generated by *Origin* software shown as an inset. As expected the presence of an increased amount of oxygen gave an increased signal intensity at  $m/z = 28$ , due to the formation of  $\text{CO}^-$  species. Furthermore, the normalized signal ratio 28/24 is approximately proportional to the ratio 16/24, so that for any given 16/24 ratio recorded from a sample, the signal arising from  $\text{CO}^-$  can be inferred. For any subsequent work on irradiated graphite samples, the presence of  $^{14}\text{C}$  is similarly implied by one or more species present generating a signal at  $m/z$  of 28 that is not attributable to  $\text{CO}^-$ .

### Irradiated graphite

The mean value for the ratios described above ( $n = 6$ ) calculated from six different sample surfaces of a single irradiated graphite trepan set are shown in Fig. 4; standard errors of the mean were calculated and are displayed as error bars. Data for the channel wall face sample are shown in Table 1.

Results are separated into inner brick surfaces (crosses) and channel wall face surface (square). As stated previously, an observation of deviation to the right of the line shown in Fig. 3 would infer the presence of  $^{14}\text{C}$ . Accordingly the data clearly show that, for this sample set, there is a significant difference between the  $^{14}\text{C}$  content on the channel wall face compared to the inner brick slices; the result is anticipated as being a true result as the data were recorded from six different areas of the same sample surface but give rise to relatively small error values. With use of the deviation from the line an approximate  $^{14}\text{C}$  concentration of  $29 \pm 4$  ppm was calculated.

This is performed under the assumption that the  $^{12}\text{C}$  signal is constant, by measuring the deviation from the line and converting to parts per million. This value was then corrected for nitrogen contribution by multiplying by the factor calculated in equation 2. Uncertainty analysis was performed by calculating the standard error of the mean for the

individual datasets and combining this with the uncertainties associated with the regression analysis in Fig. 3. The  $^{14}\text{C}$  contents of the inner brick slices, when compared to the virgin PGA, were indistinguishable, suggesting that  $^{14}\text{C}$  contents were below the limits of detection for the MS-SIMS instrument. Subsequent electron imaging of the irradiated graphite surfaces showed the presence of a surface deposit on the channel wall face (Fig. 5a) that was not found on the inner brick slices, (Fig. 5b). This is consistent with previous observations (Heard *et al.*, 2014) made from other trepanned samples extracted from the Oldbury reactor core.

## Discussion

Primarily, the present work has aimed to validate the use of MS-SIMS to investigate possible

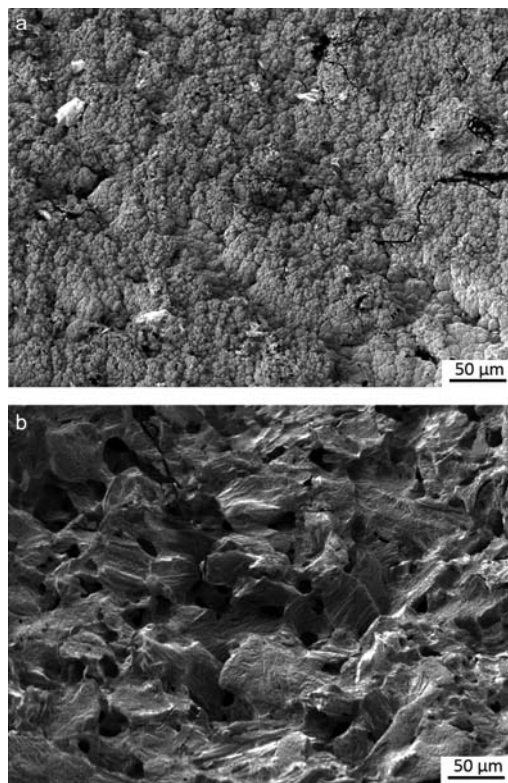


FIG. 5. (a) Electron micrograph showing the carbonaceous deposit found on a channel wall face of irradiated graphite. (b) Electron micrograph showing the structure of inner brick (non-channel wall face) of irradiated graphite.

variations in the distribution and concentration of  $^{14}\text{C}$  within irradiated graphite trepanned from a Magnox reactor core, both within the same sample set and between sample sets removed from different reactor locations. There are several operational difficulties with the use of SIMS on such samples, including the non-uniformity of the surface and the difficulty of handling active samples. However, one of the greatest challenges with this technique is the presence of isobaric interferences. For this reason it was not possible on the present instrument to use the  $m/z = 14$  signal to detect  $^{14}\text{C}$ , and so the signals at  $m/z = 24$  and  $28$  for  $^{12}\text{C}_2^-$  and  $^{14}\text{C}_2^-$  respectively were used instead. The signal at  $m/z = 28$  was also subject to isobaric interferences from species including  $^{12}\text{C}^{16}\text{O}^-$ ,  $^{14}\text{CN}^-$ ,  $^{28}\text{Si}^-$ ,  $^{13}\text{C}^{15}\text{N}^-$  and  $^{13}\text{C}^{14}\text{N}^1\text{H}^-$ . Previous work (Heard *et al.*, 2014) examining irradiated graphite samples trepanned from Oldbury using energy-dispersive X-ray spectroscopy (EDX) showed there is no evidence to suggest the presence of silicon or nitrogen in the carbonaceous coating. A correction for nitrogen contribution was also performed based on the signal arising at  $m/z = 26$  ( $^{12}\text{C}^{14}\text{N}$ ) compared to  $^{12}\text{C}_2^-$ . Additionally, as both  $^{13}\text{C}^{15}\text{N}$  and  $^{13}\text{C}^{14}\text{N}^1\text{H}$  contain minor isotopes their abundance is expected to be low, with no suggestion as to why they would be concentrated in the channel wall face deposit compared to inner brick slices. The remaining species of concern was  $^{12}\text{C}^{16}\text{O}^-$ , the interference from this fragment has been studied with the use of un-irradiated (virgin) PGA graphite exposed to increasing amounts of oxygen under vacuum in order to provide a means of subtracting this effect. It is believed that the behaviour of the deposit and PGA graphite when exposed to oxygen is similar, as EDX data show that the elemental chemistry is the same with just morphological differences (Heard *et al.*, 2014). Comparison between samples was performed with the calculation of the signals at  $m/z = 28$  and  $16$  normalized to  $m/z = 24$ , which was assumed to be constant. The  $28/24$  ratio was found to be linearly related to the  $16/24$  ratio in virgin material due to the  $\text{CO}^-$  species.

These results were subsequently used to account for the  $\text{CO}^-$  signal in the irradiated samples and to infer the  $^{14}\text{C}$  concentration. Using this technique, analysis of irradiated material showed that the channel wall face of this single trepan set appears to have an increased  $^{14}\text{C}$  concentration of  $29 \pm 4$  ppm. By comparison  $^{14}\text{C}$  in the inner brick slices was below the limits of detection for this method. The limit of detection is primarily a function of uncertainties in the regression analysis combined

with uncertainties in individual datasets and is currently estimated as approximately 2–5 ppm.

## Conclusions

The present work has successfully shown that there is a potential use of MS-SIMS to investigate relative  $^{14}\text{C}$  distributions in irradiated graphite from a Magnox reactor in the UK. Although there are limitations in the method, due to limits of detection, it has been shown that there is possible enrichment of  $^{14}\text{C}$  on exposed channel wall surfaces which is attributed to the carbonaceous deposit formed during the reactor's operating lifetime (Heard *et al.*, 2014). This work aimed at investigating the technique and developing a methodology on a single sample set; future work will examine numerous trepan sets extracted from various core locations within Reactor One of Oldbury Magnox power station using the method described in this work.

## Acknowledgements

The authors would like to thank Magnox Ltd. for their support. This work was funded by EPSRC and the Radioactive Waste Management in the UK under the GeoWaste contract.

## References

- Baston, G.M.N., Marshall, T.A., Otlet, R.L., Walker, A.J., Mather, I.D. and Williams, S.J. (2012) Rate and speciation of volatile carbon-14 and tritium releases from irradiated graphite. *Mineralogical Magazine*, **76**, 3293–3302.
- Baston, G.M.N., Preston, S., Otlet, R.L., Walker, J., Clacher, A., Kirkham, M. and Swift, B. (2014) *Carbon-14 Release from Oldbury Graphite*. AMEC/5352/002 Issue 3
- Heard, P.J., Feeney, K.A., Allen, G.C. and Shewry, P.R. (2002) Determination of the elemental composition of mature wheat grain using a modified secondary ion mass spectrometer (sims) *The Plant Journal*, **30**, 237–245.
- Heard, P.J., Payne, L., Wootton, M.R. and Flewitt, P.E.J. (2014) Evaluation of surface deposits on the channel wall of trepanned reactor core graphite samples. *Journal of Nuclear Materials*, **445**, 91–97.
- Lee, J.S., Gilmore, I., Seah, M. and Fletcher, I. (2011) Topography and field effects in secondary ion mass spectrometry – part i: Conducting samples. *Journal of The American Society for Mass Spectrometry*, **22**, 1718–1728.

- Magee, C.W. and Honig, R.E. (1982) Depth profiling by SIMS – depth resolution, dynamic range and sensitivity. *Surface and Interface Analysis*, **4**, 35–41.
- NDA [Nuclear Decommissioning Authority] (2012) *Geological Disposal. Review of Baseline Assumptions Regarding Disposal of Core Graphite in a Geological Disposal Facility*.
- NDA [Nuclear Decommissioning Authority] (2013) *Higher Activity Waste, the Long-term Management of Reactor Core Graphite Waste Credible Options (Gate a)*, SMS/TS/D1-HAW-6/002/A
- NDA [Nuclear Decommissioning Authority] (2014) *The 2013 UK Radioactive Waste Inventory. Waste Quantities from all Sources*. NDA/ST/STY(14)0010.
- Takahashi, R., Toyahara, M., Maruki, S., Ueda, H. and Yamamoto, T. (1999) Investigation of morphology and impurity of nuclear grade graphite, and leaching mechanism of carbon-14. Pp. 18–20 in: *Proceedings of the Nuclear Graphite Waste Management. Proceedings of the IAEA Technical Committee Meeting*.